Population Balance Modeling for Bubble Columns Operating in the Homogeneous Regime

M. R. Bhole and J. B. Joshi
Dept. of Chemical Engineering, Institute of Chemical Technology, University of Mumbai, Matunga, Mumbai 400 019, India

D. Ramkrishna
School of Chemical Engineering, Purdue University, West Lafayette, IN 47907

DOI 10.1002/aic.11099
Published online February 5, 2007 in Wiley InterScience (www.interscience.wiley.com).

A population balance model is developed for the prediction of the average gas holdup and axial gas holdup profile in the bubble columns operating in the homogeneous regime. The model takes into account the effect of bubble expansion along the column height and thus it is applicable to tall columns such as flotation columns in the mineral processing industries. The model captures the effect of superficial gas and liquid velocities, bubble rise velocity, operating pressure, and column height on the gas holdup. In the case of flotation columns, because of the presence of surfactants in the liquid phase, froth is observed at the top of the column. Typically, froth shows the axial profile of gas holdup and the mean bubble size, indicating that the coalescence is an important phenomenon to describe the dynamics of the froth. A probabilistic perspective is developed to address the bubble coalescence process occurring in the froth and the bubble transition probability for coalescence is obtained from experimental data in the literature. © 2007 American Institute of Chemical Engineers *AIChE J,* 53: 579–588, 2007

Introduction

Bubble column reactors are used in a variety of industrial processes for gas–liquid or gas–liquid–solid contacting. As a result of the complexities of multiphase turbulent flows, the rates of momentum heat and mass transfer in bubble columns cannot be predicted from first principles. The design procedures primarily rely on empirical or semiempirical rules. A large number of correlations have been reported in the published literature for the prediction of average gas holdup, heat and mass transfer coefficients, dispersion coefficient, and the like. However, these correlations lack generality and thus predictions for the unknown gas–liquid systems become difficult. For instance, the average gas holdup in the bubble column at superficial gas velocity of 40 mm/s is reported in the range of 5 to 40%.[1] The hydrodynamics of bubble columns depend on such operating parameters as superficial gas and liquid velocities and pressure; column dimensions such as column diameter and height to diameter ratio; the characteristics of sparging devices; and the physicochemical properties of gas and liquid phases such as density, viscosity, surface tension, and the presence of surface-active contaminants in the liquid phase—the number of variables affecting the hydrodynamics is thus very large.

Typically the empirical correlations developed for bubble columns are applicable for a specific regime of operation only. Depending on the nature of gas–liquid dispersion, the bubble columns operate in the homogeneous or heterogeneous regime. The homogeneous regime is characterized by uniformity of properties of gas–liquid dispersion across the column cross section and thus the holdup and liquid velocity profiles are indeed flat. The bubble size is almost uniform, with mean bubble diameter generally not exceeding 5 mm. The length scale of the turbulence is of the order of bubble diameter. Such a

Correspondence concerning this article should be addressed to D. Ramkrishna at ramkrish@ecn.purdue.edu.

regime is generally observed at lower superficial gas velocities (<50 mm/s). At higher superficial gas velocities, the column generally operates in the churn-turbulent regime (heterogeneous regime), which is characterized by liquid circulation and a radial gas holdup profile. The vortical structures in the form of circulation cells span the entire column and thus the length scale of the turbulence is of the order of column dimensions. A wide bubble size distribution exists that is governed by the relative magnitudes of bubble coalescence and breakup rates.

For successful design of bubble columns, a thorough understanding of fluid mechanics of gas–liquid flows is required. The mechanics of gas–liquid flow is profoundly dependent on the bubble size. Depending on the bubble size, their rise velocities can vary from 50 to 500 mm/s. The bubble size appreciably affects the gas holdup. Further, the bubble shape is also dependent on its size. Generally the small-sized bubbles having diameter < 2 mm are spherical and they rise in rectilinear paths. The shapes of large-diameter bubbles can be ellipsoidal or spherical cap and they may exhibit a wobbling motion.[2] Obviously, bubble size also affects the interfacial area available for gas–liquid mass transfer.

Because of the fundamental importance of bubble size in gas–liquid flows, the predictions of bubble size distribution become very important for the understanding of the hydrodynamics of bubble columns. When the bubble coalescence and breakup are insignificant, the bubble size distribution and thus the mean bubble size are governed by the sizes of the bubbles generated at the gas sparging device and their velocities through the column. This is typically the situation for the homogeneous regime of operation of bubble columns. On the other hand, when the bubble coalescence and breakup are significant, the evolution of the bubble size distribution is also governed by the relative magnitudes of bubble coalescence and breakup rates. Population balance modeling offers a natural framework for such considerations.[3–6] In this work, we have focused primarily on the prediction of the gas holdup profile and the average gas holdup in a bubble column reactor based on population balance modeling. Herein we consider the case of bubble columns operating in the homogeneous regime with no bubble coalescence and breakup. The model developed is tested for the data from the literature where the bubble coalescence and breakup are indeed negligible. Such a simple model is able to capture the dependency of gas holdup on such variables as superficial gas and liquid velocities, bubble rise velocity, operating pressure, and column height.

Population Balance Model for the Homogeneous Regime

The homogeneous regime is obtained when the superficial gas velocity in the column is low (typically <50 mm/s) and the gas sparging is uniform over the column cross section. Further, the sizes of the bubbles generated at the sparger need to be small. The presence of surface-active components, which prevent bubble coalescence, extends the stability of a homogeneous regime. The objective is to determine the gas holdup in the column. The model presented here builds on basic features of a preliminary formulation for gas holdup, presented by Ramkrishna.[6] Accordingly, we consider a simple one-dimensional (axial) flow of the gas and liquid in a bubble column. Because ideal bubbly flow is assumed, the bubbles rise without interacting with each other. Also no random bubble motion is assumed in this development. As the bubbles rise along the column axis, they expand as the result of a reduction in the hydrostatic head in accordance with the ideal gas law. The bubbles generated at the sparger eventually reach the column top where they disengage from the liquid phase. Bubbles approaching a gas–liquid interface at the top are slowed down by a draining film so that this could have an effect on the gas holdup. Typically, froth is formed in the bubble columns containing surfactants in the liquid phase. Bubble coalescence is an important aspect of hydrodynamics of the froth. A probabilistic perspective is developed to address the bubble coalescence and to explain the experimental observations of Yianatos et al.[7]

Population Balance Model without Bubble Retardation Effect at the Top

Let the expected number of bubbles with volume between x and $x + dx$, at height (axial location) between z and $z + dz$ be $f_1(x, z)dxdz$. Given that at any axial location z, bubble distribution is assumed to be independent of location along a given cross section, the number density function f_1 may be regarded as averaged over the cross section of the column. Because the bubble column is assumed to be operated at steady state, time does not appear in the number density function. In the absence of bubble coalescence and breakup, the population balance equation is given by

$$\frac{\partial}{\partial x}\left[\dot{X} f_1(x,z)\right] + \frac{\partial}{\partial z}\left[\dot{Z} f_1(x,z)\right] = 0 \tag{1}$$

where $\dot{X}$ and $\dot{Z}$ are the velocities along the x and z coordinates, respectively. $\dot{X}$ represents the rate at which the bubble volume increases, whereas $\dot{Z}$ represents the bubble rise velocity with respect to stationary coordinates. The boundary condition for Eq. 1 is obtained by requiring that

$$f_1(x,0) = N_0 f(x) \tag{2}$$

where N_0 is the total number density and $f(x)$ is the size distribution of the bubbles emerging from the sparger.

The bubble rise velocity with respect to stationary coordinates $\dot{Z}$ is the sum of the local liquid velocity and bubble slip velocity. The bubble slip velocity is not an entirely well characterized quantity because it is influenced by the presence of neighboring bubbles. For monodisperse systems, the slip velocity is related to the terminal rise velocity by the Richardson–Zaki correlation, which characterizes the hindrance effect for the multiphase dispersion.[8] However, for the present, we make a simplification that the bubble slip velocity is equal to the terminal rise velocity and is a simple function of bubble volume. Incorporation of the hindrance effect in the population balance model is performed at a subsequent stage. Thus, for now we set

$$\dot{Z} = u_L + Ax^b \tag{3}$$

Here Ax^b is the terminal bubble rise velocity, where A and b are constants depending on the drag law used to describe the motion of a single bubble in the stagnant liquid. For example, the value of b is 2/3 when the drag coefficient is specified by Stokes' law, whereas b is 1/6 according to the Davies–Taylor law.[2]

Because we are concerned with one-dimensional flow, bubble rise velocity and liquid velocity can be regarded as averaged over the column cross section. Thus, in the absence of net liquid flow, the liquid velocity at any location in the column is zero. When the net liquid throughput is present, as in the case of cocurrent or countercurrent bubble columns, then the local liquid velocity can be considered as the cross-section–averaged interstitial liquid velocity. To facilitate an analytical solution to the population balance equation, we consider the simplest case whereby the value of local liquid velocity is constant at any axial location and is given as

$$u_L = V_L/\overline{\in}_L \tag{4}$$

where V_L is superficial liquid velocity and $\overline{\in}_L$ is the average liquid holdup in the column, given by

$$\overline{\in}_L = \frac{H_0}{H} \tag{5}$$

where H_0 is the clear liquid height, which is the height of liquid column in the absence of gas throughput, and H is the height of gas–liquid dispersion. Our objective is to find out the average gas holdup or the height of dispersion H for a given H_0 and the phase flow rates.

To obtain the rate at which the bubble volume increases ($\dot{X}$), we use the ideal gas law. The bubbles expand as they rise in the column as the result of a reduction in the hydrostatic head. At constant temperature and assuming no mass transfer from gas to liquid, we can express the bubble volume at any axial location z as follows:

$$x = x_0\left[\frac{H_a + H_0}{H_a + H_0 - z\ (H_0/H)}\right] \tag{6}$$

Here H_a is the pressure head acting on the top of the column ($H_a = P_0/\rho_L g$). To obtain the analytical solution for Eq. 1 using the method of characteristics, we recognize that z itself can be used as a variable along the characteristic. Thus,

$$\frac{dx}{dz} = \frac{\dot{X}}{\dot{Z}} \tag{7}$$

From Eqs. 6 and 7, the rate at which bubble volume increases can be obtained as follows:

$$\dot{X} = \frac{x(H_0/H)\dot{Z}}{H_a + H_0 - z(H_0/H)} \tag{8}$$

Equation 1 is now integrated along the characteristic. Recognizing that $d\dot{Z}/dz = 0$, the number density function can be obtained, after some simplifications, as

$$f_1(x,z) = N_0 f(x_0)\left[\frac{H_a + H_0 - z\ (H_0/H)}{H_a + H_0}\right]^{b+1} \times \left\{\frac{u_L + Ax_0^b}{u_L\left[\frac{H_a+H_0-z(H_0/H)}{H_a+H_0}\right]^b + Ax_0^b}\right\} \tag{9}$$

The height of the gas–liquid dispersion H is, in fact, unknown and can be obtained from the mass balance on the gas phase:

$$H - H_0 = \int_0^\infty x dx \int_0^H f_1(x,z) dz \tag{10}$$

By substituting the solution for the number density function from Eq. 9 and introducing the transformation from Eq. 6, the following expression for the gas holdup is obtained:

$$\overline{\in}_G = \frac{H - H_0}{H} = \frac{\phi_0}{b}\left(\frac{H_a + H_0}{H_0}\right)\left(\frac{V_L/\overline{\in}_L + A\overline{x}_0^b}{V_L/\overline{\in}_L}\right) \times \ln\left\{\frac{V_L/\overline{\in}_L + A\overline{x}_0^b}{V_L/\overline{\in}_L[H_a/(H_a + H_0)]^b + A\overline{x}_0^b}\right\} \tag{11}$$

In deriving Eq. 11 it is assumed that the monosized bubbles of size $\bar{x}_0$ are generated at the sparger. Thus, the bubble size distribution emerging from the sparger is described by a Dirac-delta function:

$$f(x_0) = \delta(x_0 - \bar{x}_0) \tag{12}$$

Further, we have set $\phi_0 = N_0\bar{x}_0$ for the volume fraction of the gas at the sparger. It can be seen that Eq. 11 must be solved iteratively to obtain the average gas holdup.

The average superficial gas velocity in the column can be obtained as

$$V_G = \frac{G}{(\rho_G)_{avg}} \tag{13}$$

where G is the mass flux of the gas at any location z in the column, which is given by

$$G(z) = \int_0^\infty \rho_G x f_1(x,z)\dot{Z} dx \tag{14}$$

By substituting the expression for the number density and gas velocity from Eqs. 9 and 3 and introducing the transformation of variable from Eq. 6, the following expression is obtained for the gas mass flux:

$$G(z) = \rho_G\phi_0(A\overline{x}_0^b + u_L)\left(\frac{H_a + H_0}{H_a + H_0 - zH_0/H}\right) \tag{15}$$

Because the density of gas at any axial height z is proportional to the total pressure at that point $\{\rho_G\alpha[H_a + H_0 - z(H_0/H)]\}$, Eq. 15 indicates that the gas mass flux is (as it should be) independent of axial location in the column. The following expression for the superficial gas velocity is obtained:

$$V_G = \phi_0(u_L + A\overline{x}_0^b)\left(\frac{H_a + H_0}{H_a + H_0/2}\right) \tag{16}$$

The gas holdup at the sparger (ϕ_0) is not an easily accessible quantity. Further, most of the data on the homogeneous regime are in the form of average gas holdup vs. superficial gas velocity. Thus, ϕ_0 can be eliminated from Eqs. 11 and 16 and the average gas holdup can be obtained as a function of superficial gas velocity as follows:

$$\overline{\in}_G = \frac{V_G}{b}\left(\frac{H_a + H_0/2}{H_0}\right)\left(\frac{1}{V_L/\overline{\in}_L}\right) \times \ln\left\{\frac{V_L/\overline{\in}_L + A\overline{x}_0^b}{(V_L/\overline{\in}_L)[H_a/(H_a+H_0)]^b + A\overline{x}_0^b}\right\} \quad (17)$$

Equation 17 describes the $\overline{\in}_G$ vs. V_G relationship for a continuous bubble column operating in the homogeneous regime. The value of b can be obtained from the drag law that governs the bubble motion as shown later. It is interesting to observe that Eq. 17 allows a comparison of model prediction to data available in the literature in spite of the uncertainty associated with the bubble size at the sparger and the bubble velocity at the sparger (and elsewhere) in the column. This is accomplished by demanding consistency with directly fitting the bubble velocity at the sparger without having to individually resolve the values of A, b, and $\bar{x}_0$.

For the bubble column operating in the semibatch mode, the liquid velocity $u_L = 0$. In this case, the population balance model (Eq. 1) can be solved using the method of characteristics in a similar manner to yield the following expressions, respectively, for the number density, average gas holdup, and superficial gas velocity:

$$f_1(x,z) = N_0 f(x_0)\left(\frac{H_a + H_0 - z(H_0/H)}{H_a + H_0}\right)^{b+1} \quad (18)$$

$$\overline{\in}_G = \frac{\phi_0}{b}\left(\frac{H_a + H_0}{H_0}\right)\left[1 - \left(\frac{H_a}{H_a + H_0}\right)^b\right] \quad (19)$$

$$V_G = \phi_0(A\overline{x}_0^b)\left(\frac{H_a + H_0}{H_a + H_0/2}\right) \quad (20)$$

Thus, for the semibatch bubble column,

$$\overline{\in}_G = \frac{V_G}{A\overline{x}_0^b}\left(\frac{H_a + H_0/2}{H_0 b}\right)\left[1 - \left(\frac{H_a}{H_a + H_0}\right)^b\right] \quad (21)$$

It must be noted that Eq. 21 can also be obtained by taking the limit of Eq. 17 as $V_L \to 0$. Obviously, the semibatch bubble column can be considered as a special case of continuous bubble column with superficial liquid velocity equal to zero.

The atmospheric pressure head $H_a \cong 10.33$ m of water column. Generally, the height of the liquid column H_0 in a typical laboratory experiment is about 1 m. Under these circumstances, the increase in the bubble volume as bubbles rise from the sparger to the top is negligible and thus the bubble rise velocity is also practically identical everywhere in the column and is equal to the rise velocity of the bubbles at the sparger. It has been assumed here that the bubble reaches its steady-state rise velocity immediately at the sparger ($z = 0$) where it is formed. In this case, the average gas holdup and superficial gas velocity can be obtained from Eqs. 19 and 20 by taking the limit $(H_0/H_a) \to 0$, which gives

$$\overline{\in}_G = \phi_0 \quad (22)$$

$$V_G = \phi_0(A\overline{x}_0^b) \quad (23)$$

Thus the average gas holdup in the column is the same as the gas holdup at the sparger and the (constant) bubble rise velocity is equal to the ratio of superficial gas velocity to average gas holdup in the column. This is an obvious result for the bubble columns operating in the homogeneous regime with a constant bubble size throughout the column. The population balance model developed in this work essentially captures this result as a special case.

The gas holdup at any height z in the column can be obtained as

$$\in_G(z) = \int_0^\infty x f_1(x,z)\,dx \quad (24)$$

By substituting for the number density from Eq. 18 and using the transformation from Eq. 6, the following result is obtained:

$$\in_G(z) = \phi_0\left(\frac{H_a + H_0 - z(H_0/H)}{H_a + H_0}\right)^{b-1} \quad (25)$$

Figure 1 shows the evolution of gas holdup along the column height in a semibatch bubble column for different values of b. As the bubbles rise in the column they expand, which tends to increase the gas holdup. However, as the bubble size increases, the rise velocity also increases, resulting in a reduction in the residence time of the bubbles in the column and thus tending to decrease the gas holdup. The overall effect of these two factors on the gas holdup depends on the value of constant b. The model predicts an increase in the gas holdup along the column height when $b < 1$ and a decrease in the gas holdup along the column height when $b > 1$. At $b = 1$, the gas holdup remains the same at any location in the column, its value being equal to the value of gas holdup at the sparger. The value of constant b depends on the drag law that governs the steady-state motion of a bubble in stagnant liquid and is usually dependent on the bubble size itself. When Stokes' law is used to describe the steady-state motion of a single bubble, $b = 2/3$. However, it is applicable only for very fine bubbles having Reynolds number $\ll 1$. The homogeneous regime in bubble columns is typically characterized by the bubbles having diameter between 1 and 5 mm. It is difficult to specify the rise velocity as a function of bubble diameter in this range. For example, a bubble of diameter 2 mm can have a rise velocity anywhere from 0.15 to 0.30 m/s.[2] Depending on the presence of surface-active contaminants at the gas–liquid interface and deformation of bub-

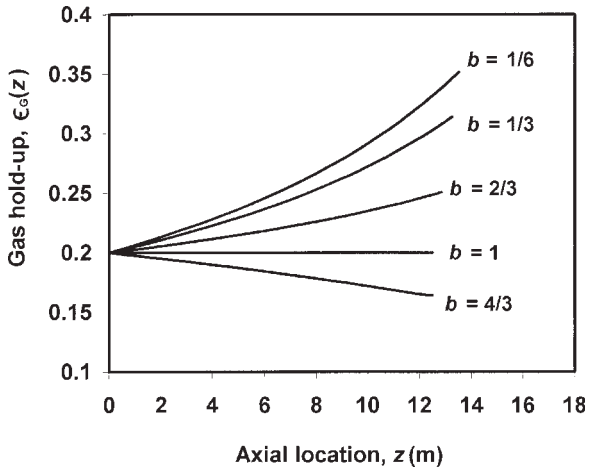

Figure 1. Variation of gas holdup along the column height for different values of b.

$H_0 = 10$ m, $\phi_0 = 0.2$.

bles, the bubble rise velocity can vary over a wide range and thus the value of b can be anywhere from 0 to 0.5 for practical cases in bubble columns. For pure liquids (having no surface active contaminants) and for a certain range of bubble diameters, the rise velocity can even decrease with an increase in the bubble size.[9] However, in all the cases the value of constant b is <1 and thus the gas holdup can increase only with an increase in the column height in the bubble column operating in the homogeneous regime in the absence of bubble coalescence and breakup.

Experimental measurements by Gomez et al.,[10] Zhou and Egiebor,[11] and Yianatos et al.[12] support this result. Gomez et al.[10] reported an increase of roughly 100% in the gas holdup from the bottom to the top of the collection zone in the flotation column of height 10 m. Typically, the collection zone in the flotation column is known to operate in the homogeneous regime. Figure 2 shows a comparison of the axial gas holdup profile measured by Zhou and Egiebor[11] with the predictions of the model developed in this work. A consistent increase in the gas holdup with the column height is essentially captured by the model. It must be noted that the increase in gas holdup along the column height becomes significant only for the tall columns. For typical laboratory bubble columns of height of the order of 1 m, the increase in the gas holdup along the column height is negligible for all practical purposes.

Figure 3 shows the predictions of Eq. 21 for the average gas holdup with the rise velocity of the bubbles generated at the sparger ($A\bar{x}_0^b$) as a parameter for the semibatch bubble column. The $\overline{\in}_G$ vs. V_G relationship is seen to be linear, as expected, for the homogeneous regime. Further, the gas holdup decreases with an increase in the rise velocity of the bubbles. As the bubble rise velocity increases, the residence time of the bubbles in the column decreases, thus resulting in a decrease in the gas holdup.

With an increase in the operating pressure, the gas holdup also increases. However, the effect of pressure is also dependent on regime of operation. At high pressure, bubble coalescence is suppressed and small bubbles are formed as a result of the instability of large bubbles.[13] Thus there is a substantial increase in the gas holdup with an increase in the pressure when the bubble column is operating in the heterogeneous regime.[13,14] However, for the homogeneous regime, in the absence of bubble coalescence, breakup, and liquid flow pattern, the effect of pressure on the gas holdup is expected to be minimal. This is indeed evident from the measurements of gas holdup at low superficial gas velocities (whereby the homogeneous regime is ensured) carried out by Wilkinson[13] and Letzel[14] at various operating pressures. By varying the quantity H_a in Eq. 21, the effect of pressure on the gas holdup can be observed. When the top of the column is open to the atmosphere, H_a represents atmospheric pressure head, which is 10.33 m of the water column. Thus an increase in H_a represents the increase in operating pressure. Although the gas holdup is seen to increase with the pressure from Figure 4, the effect of pres-

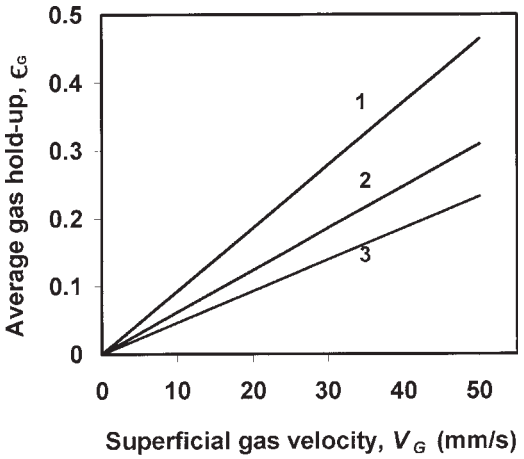

Figure 3. Variation of average gas holdup with superficial gas velocity for different terminal bubble rise velocities.

1: $A\bar{x}_0^b = 0.10$ m/s; 2: $A\bar{x}_0^b = 0.15$ m/s; 3: $A\bar{x}_0^b = 0.20$ m/s; $H_0 = 10$ m, $b = 1/3$.

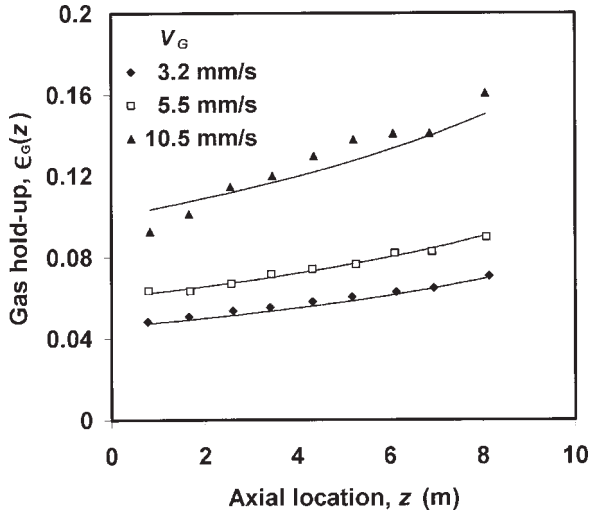

Figure 2. Comparison of predictions of Eq. 25 (b = 1/6) with the gas holdup data in a laboratory-scale flotation column of height 9.5 m.

Data from Zhou and Egiebor.[11]

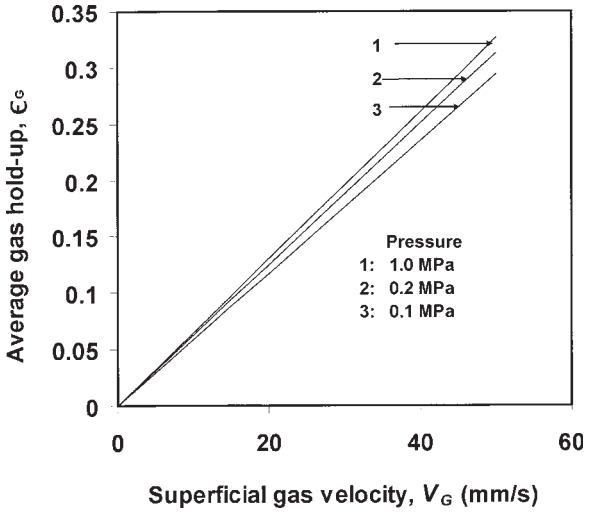

Figure 4. Variation of average gas holdup with superficial gas velocity for different operating pressures.

$H_0 = 10$ m, $b = 1/3$, $A\bar{x}_0^b = 0.15$ m/s.

sure is not very significant. Further, for the bubble column where the height of the liquid column H_0 is much less than the pressure head on the top (H_a), the gas holdup is virtually constant and is independent of pressure.

Until now, we have considered bubble slip velocity to be equal to the bubble rise velocity. In other words, the hindrance effect was neglected. Apart from bubble volume, slip velocity is also dependent on the local gas holdup. For monodispersed gas–liquid systems, the Richardson–Zaki-type correlation[8] can be used for the estimation of bubble slip velocity:

$$V_s = (Ax^b)\, \in_L^{m-1} . \tag{26}$$

We use the average liquid holdup instead of local liquid holdup in Eq. 26 for the estimation of slip velocity. This is not a drastic simplification for a bubble column operating in the homogeneous regime, especially when the column height is not large, so that the local liquid holdup is practically identical to the average liquid holdup in the column. Because the average liquid holdup is a constant (although unknown), it eliminates the spatial dependency of slip velocity. Thus the bubble velocity with respect to stationary coordinates is given by

$$\dot{Z} = u_L + (Ax^b)\overline{\in}_L^{m-1} \tag{27}$$

The population balance equation (Eq. 1) can be solved in conjunction with Eq. 27 and the expressions for the average gas holdup and superficial gas velocity can be obtained. For the case of a semibatch bubble column, the average gas holdup is given as

$$\overline{\in}_G = \frac{V_G}{A\bar{x}_0^b \overline{\in}_L^{m-1}} \left(\frac{H_a + H_0/2}{H_0 b}\right) \left[1 - \left(\frac{H_a}{H_a + H_0}\right)^b\right] \tag{28}$$

A problem arises, however, with the estimation of m, which is the Richardson–Zaki index, for which various investigators have reported different values. The value of m is known to vary from 1 to 2.4 for the bubble columns.[15] In the case of monodispersed solid particles in the liquid or gas phase, the Richardson–Zaki index can be defined based on the particle Reynolds number. However, the behavior of bubbles can be dramatically different from that of solid particles. The gas–liquid interface can be regarded as rigid when the surface-active impurities are present at the interface and the behavior of the bubbles is similar to that of solid particles. The bubbles in a pure liquid exhibit a partially mobile gas–liquid interface. Because it is difficult to characterize the extent of contamination of the gas–liquid interface, estimation of the Richardson–Zaki index also becomes difficult. In this work, we have assumed that the value of m is given. Figure 5 shows $\overline{\in}_G$ vs. V_G variation for the semibatch bubble column for the various values of Richardson–Zaki index. It is seen that for a given superficial gas velocity, the gas holdup increases with an increase in the value of m. This is obviously expected because the value m characterizes the hindered motion of bubbles. As the value of m increases, the bubble velocity with respect to fixed coordinates decreases, leading to an increase in the gas holdup. From Figure 5, it is also seen that the linearity of the $\overline{\in}_G$ vs. V_G relationship is valid only for unhindered bubble motion for which $m = 1$.

Figures 6A and 6B show $\overline{\in}_G$ vs. V_G variation for various values of superficial liquid velocities. The value of superficial liquid velocity is considered negative or positive depending on the countercurrent or cocurrent mode of gas–liquid flows, respectively. Thus, for a given value of bubble slip velocity, the bubble velocity with respect to stationary coordinates is higher for cocurrent flow than that for countercurrent flow. This explains the observed gas holdup behavior. The average gas holdup is higher for a countercurrent bubble column. Schugerl et al.[16] observed that the superficial liquid velocity does not affect the average gas holdup in the homogeneous regime. On the other hand, Finch and Dobby[17] observed that the gas holdup is appreciably affected by the superficial liquid velocity. The observations of both groups can be explained by the model developed in this work. Equation 17 predicts that the effect of superficial liquid velocity on the average gas holdup diminishes as the value of bubble slip velocity increases, which is evident from Figures 6A and 6B. Finch and Dobby[17] obtained the gas holdup data from the laboratory flotation column. They used a ceramic sparger, which produces very fine bubbles with diameters typically not exceeding 2 mm. Further, the liquid phase contained Dowfroth 250, a frother that maintains very small bubbles in the liquid phase. Typically, the values of slip velocity in their flotation experiments were not >70 mm/s and thus the gas holdup was substantially affected by superficial liquid velocity. Figure 6A depicts this situation where the effect of superficial liquid velocity on the gas holdup is significant. On the other hand, Schugerl et al.[16] obtained the gas holdup in a fermentation column where the values of bubble slip velocity were in excess of 150 mm/s and thus the effect of superficial liquid velocity on the gas holdup was seen to be negligible. Figure 6B depicts the corresponding situation. The comparison of gas holdup data obtained by Finch and Dobby[17] with the model predictions is shown in Figure 7.

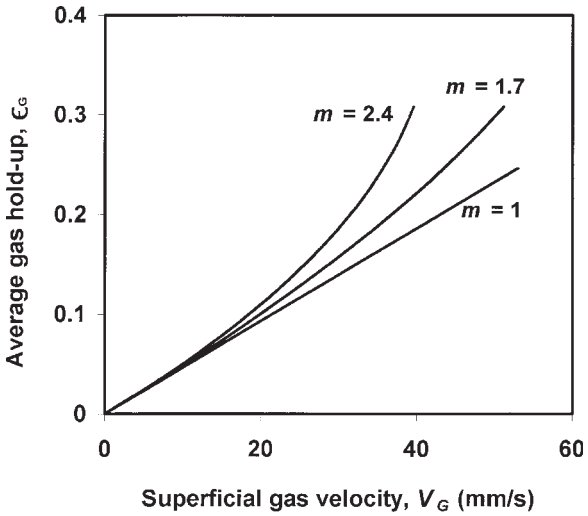

Figure 5. Variation of average gas holdup with superficial gas velocity for different values of Richardson–Zaki index.

$H_0 = 10$ m, $b = 1/3$, $A\bar{x}_0^b = 0.20$ m/s.

In a typical laboratory bubble column using air and water as dispersed and continuous phases, respectively, bubble coalescence is unavoidable even at low gas flow rates in the bubbly flow regime.[16] However, because of the presence of a frother in the liquid phase, bubble coalescence and breakup can be completely neglected in the collection zone of a typical flota-

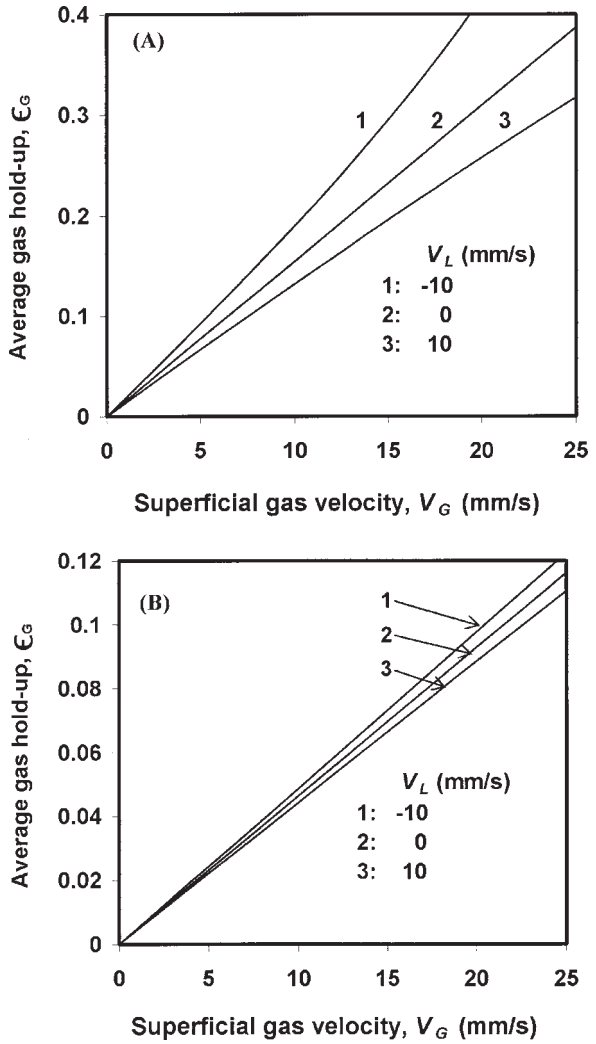

Figure 6. Variation of average gas holdup with superficial gas velocity for different values of superficial liquid velocities.

$H_0 = 10$ m, $b = 1/3$. (A) $A\bar{x}_0{}^b = 0.06$ m/s; (B) $A\bar{x}_0{}^b = 0.20$ m/s.

tion column. Thus, the flotation column also offers an opportunity to test the predictions of the model developed in this work; it is already evident from the successful predictions of the gas holdup as shown in Figures 2 and 7. Further, Figure 8 shows the comparison of the experimental gas holdup obtained by Xu and Finch[18] with the model predictions for a flotation column. These investigators used cloth spargers having different surface areas in the flotation columns. Each sparger was characterized by the quantity R_S, defined as

$$R_S = \frac{A_C}{A_S} \tag{29}$$

where A_C is the cross-sectional area of the column and A_S is the surface area of the sparger. The diameter of the bubbles produced by the sparger was correlated as

$$d_B = C_1(R_S V_G)^q \qquad (R_S < 1) \tag{30}$$

where C_1 and q are constants. Typically, $q \simeq 0.25$.[18] As the value of R_S increases, the size of the bubbles produced by the

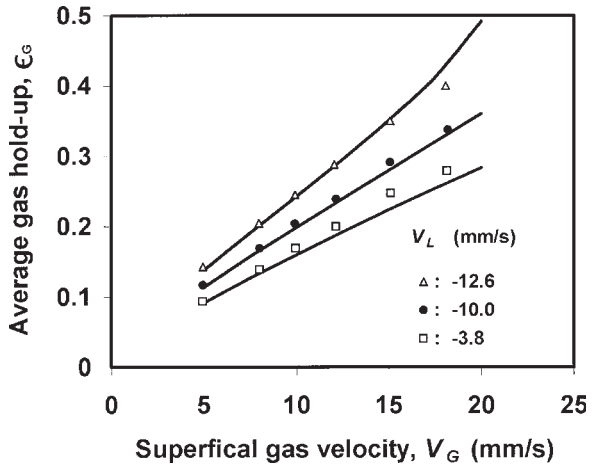

Figure 7. Comparison of the gas holdup data for countercurrent flotation column[17] with the model predictions.

particular sparger increases. This obviously leads to an increase in the bubble rise velocity in the column and the gas holdup decreases. From Figure 8, it is evident that the model essentially captures the correct trends in the gas holdup data for the spargers having different values of R_S.

Model for Froth

The population balance model for the homogeneous regime assumed bubbles to rise at their respective terminal velocities. However, the bubbles approaching a free gas–liquid interface are slowed down because of the effects of surface tension causing an increase in the gas holdup near the interface. This region near the gas–liquid free surface with relatively higher gas holdup is commonly referred to as *froth* (see Figure 9). In a continuous column, the height of the froth zone depends on the stability of the froth. When air is bubbled through ordinary tap

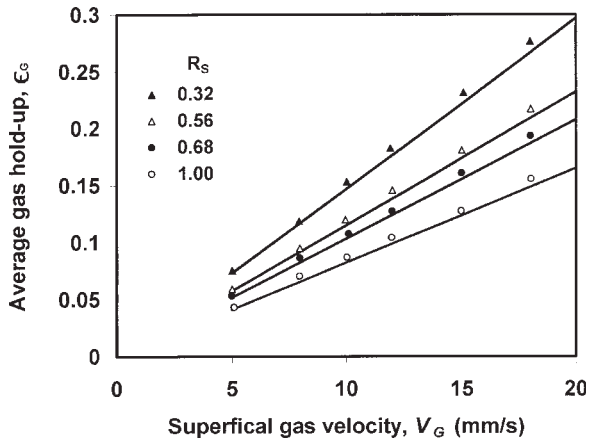

Figure 8. Comparison of the gas holdup data for countercurrent flotation column with cloth spargers of different surface areas[18] with the model predictions.

$V_L = 3$ mm/s.

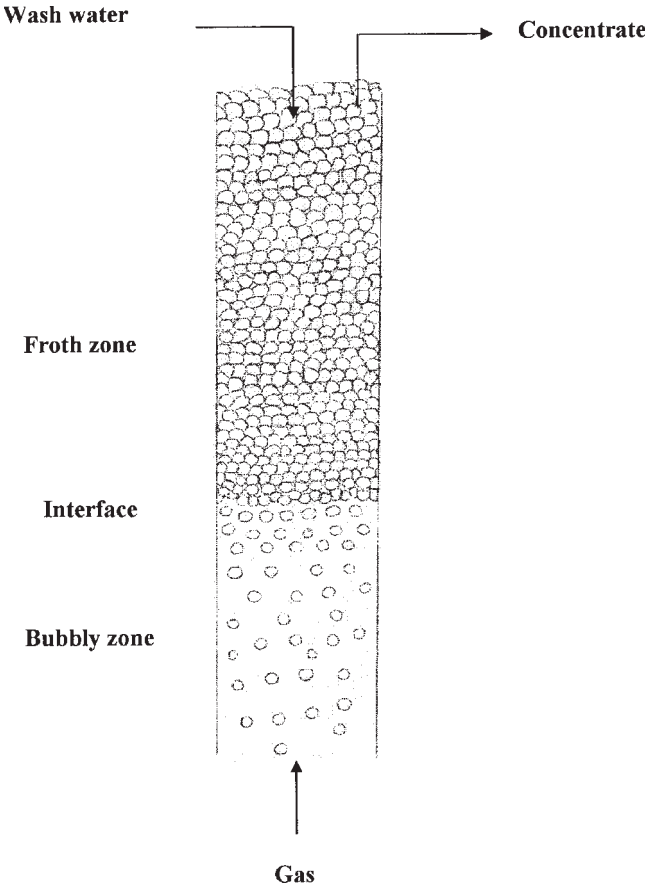

Figure 9. Schematic of froth in a typical flotation column.

water, the froth height is generally very small. However, the presence of surface-active components such as frothers stabilizes the froth and the froth height increases. In a typical continuous flotation column, a small amount of water is spread on the top of the froth and it is referred to as wash water. A part of the wash water overflows with the froth bubbles and the remaining part flows down the froth countercurrent to the gas phase. The practice of addition of "wash water" in industrial columns leads to the formation of froths that are as tall as 1 m.[17] The schematic of column froth is shown in Figure 9. The two distinct zones—the homogeneous bubbly zone and the froth zone—are separated by a clear froth–liquid interface at which there is an abrupt increase in the gas holdup to a value of roughly 60%.[7] Further, within the froth, the gas holdup increases along the height. It is also known that the bubble coalescence occurs and thus the mean bubble diameter increases along the froth height.

Mathematical Model

Admitting coalescence into a population balance model for the froth layer requires some discussion of a conceptual nature. The usual perspective of a population balance model for an aggregating population envisages particles (bubbles) with varying velocities (by one or more mechanisms) colliding with each other and aggregating (or coalescing) if an intervening film drains off before forces tending to disengage the particles succeed in doing so. A number balance is made on particles of specific sizes at each location by accounting for changes caused by particle motion as well as aggregation between particles. Such is not the scenario in a froth in which bubbles are slowly moving in a crowd of fellow bubbles with a coalescence event occurring, should two (or more) bubbles be deprived of the film separating them. Details of the hydrodynamics are complex, defying the formulation of a model with the level of simplicity that we seek. We present below how a simple population balance model can be formulated to describe coalescence in the froth layer.

Following Ramkrishna and Borwanker[19] or Ramkrishna[6], we view the steady-state coalescence process from a probabilistic perspective rather than a population balance. Before we recall this viewpoint, let us grant that the bubbles are described by volume as a single internal coordinate and spatial location at any cross section as external coordinates. The vertical coordinate z may be regarded as an *evolutionary* coordinate in that the population density is not to be regarded as a density in this variable. The bubbles are assumed to be transversely mixed by turbulent diffusive motion with zero mean velocity along the cross section and moving upward with velocity $\dot{Z}(z)$ independently of their size. This assumption may be justified in the case of a packed bed of froth bubbles where the velocity of rise of bubbles is constrained only by the rate at which the bubbles escape from the top. As the bubbles rise in the froth, their velocity decreases, leading to an increase in the gas holdup. The transverse mixing of bubbles is assumed to deprive the expected population density of any dependency on location at any cross section. The probabilistic viewpoint of the expected population density $f_1(x, z)$ may be described as $f_1(x, z)dAdx =$ Probability that there is a bubble (that is, with center) in area dA with volume in the interval $(x, x+ dx)$. The dual interpretation implies that the quantity above is also the expected number of particles with centers in the area dA and volume between x and $x + dx$. The bubble in its vertical climb with velocity $\dot{Z}(z)$ through the infinitesimal section of the column between z and $z + dz$ is likely to encounter another bubble at another location along the same cross section with which it could coalesce. The probability that a pair so located would coalesce is defined to be $\beta(z)dz$. The probability that there are two bubbles along the same cross section one in area dA with volume x, and another in a different area dA' with volume x' is assumed to be the product of the individual probabilities, which is an assumption of statistical independence. Thus by following a methodology similar to that presented by Ramkrishna and Borwanker[19] we arrive at the following integropartial differential equation:

$$\frac{\partial}{\partial z}[\dot{Z}f_1(x,z)] = \frac{\beta(z)}{2}\int_0^x f_1(x-x',z)f_1(x',z)dx' - \beta(z)f_1(x,z)\int_0^\infty f_1(x',z)dx' \qquad (31)$$

We further assume that monosized bubbles enter the froth, which of course, because of the non-size-selective coalescence prevents establishment of a distribution of bubble sizes in the froth. For nonuniform sizes in the feed to the froth section, a size distribution is not precluded, however.

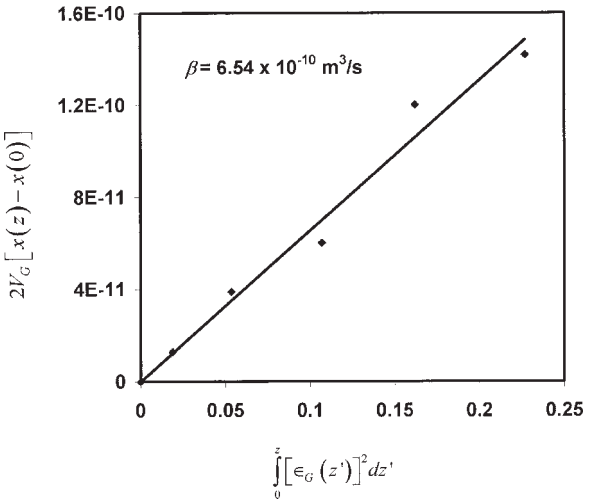

Figure 10. Determination of transition probability for bubble coalescence in the froth from the data of Yianatos et al.[7]

Note that the transition probability is obtained from the slope of the best-fit line.

To obtain the solution of Eq. 31 we define the following function:

$$g_1(x,z) = f_1(x,z)\,\dot{Z}(z) \tag{32}$$

From Eqs. 31 and 32, one can write

$$\frac{\partial}{\partial z}[g_1(x,z)] = \frac{\beta(z)}{2\,\dot{Z}^2}\int_0^x g_1(x-x',z)g_1(x',z)dx' - \frac{\beta(z)}{\dot{Z}^2}g_1(x,z)\int_0^\infty g_1(x',z)dx' \tag{33}$$

Equation 33 admits the following solution:

$$\frac{1}{\mu_0(z)} - \frac{1}{\mu_0(0)} = \frac{1}{2}\int_0^z \frac{\beta(z')}{\dot{Z}^2}dz' \tag{34}$$

We note that z' is a dummy variable in Eq. 34 and μ_0 is the zeroth moment of function $g_1(x, z)$, defined as

$$\mu_0(z) = \int_0^\infty g_1(x,z)dx = \dot{Z}(z)N_0(z) \tag{35}$$

The second equality on the right-hand side of Eq. 35 arises from the definition of zeroth moment of number density function:

$$N_0(z) = \int_0^\infty f_1(x,z)dx \tag{36}$$

where $N_0(z)$ is the total number density, that is, the number of bubbles per unit volume at location z.

Further, we note the following two relationships:

$$\dot{Z}(z) = \frac{V_G}{\in_G(z)} \tag{37}$$

$$N_0(z) = \frac{\in_G(z)}{\overline{x}(z)} \tag{38}$$

Equation 37 defines the gas velocity with respect to stationary coordinates in terms of superficial gas velocity and the local gas holdup. In Eq. 38 the total number density at any location z in the froth is expressed in terms of mean bubble volume at that location.

From Eqs. 34, 35, 37, and 38 the following expression is obtained for the variation of mean bubble volume in the froth:

$$\overline{x}(z) - \overline{x}(0) = \frac{1}{2V_G}\int_0^z \beta(z)[\in_G(z)]^2 dz \tag{39}$$

Equation 39 is an integral equation in $\beta(z)$, which is solvable as an inverse problem with due regularization. It is expected that the bubble transition probability for coalescence with other bubbles will increase as it climbs through a more packed population of bubbles. However, only limited experimental data are available for the variation of mean bubble sizes and the gas holdup in the froth that did not allow clear discrimination to obtain bubble transition probability for coalescence as a function of z. A constant value for β seems appropriate for the experimental data of Yianatos et al.[7] used in this work. The bubble transition probability for coalescence can now be obtained from the slope of the graph as shown in Figure 10. The predictions of mean bubble diameter from this model are in conformity with the experimental values as seen from Figure 11. We note that the experimental data of gas holdup were fitted as a second-order polynomial in z to enable the solution of Eq. 39 for the constant β.

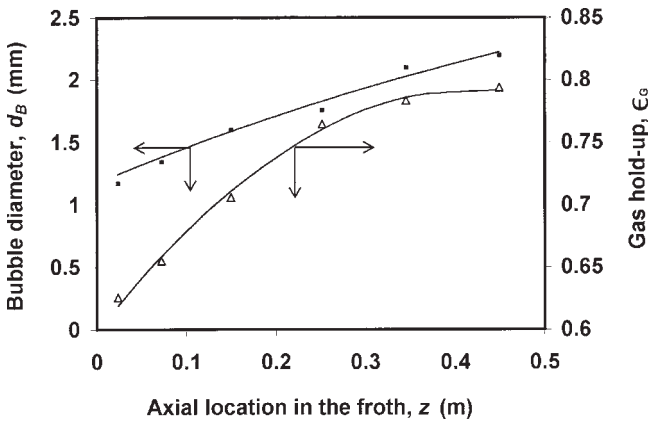

Figure 11. Predictions of the bubble coalescence model for the experimental data of Yianatos et al.[7]

△: Experimental values of the gas holdup in the froth. ■: Experimental values of the mean bubble diameter in the froth. Continuous line for bubble diameter is a prediction based on $\beta = 6.54 \times 10^{-10}$ m^3/s; continuous line for the gas holdup is a best-fit second-order polynomial in z.

Conclusions

(1) The population balance model is developed for the homogeneous regime of operation of continuous bubble column, taking into consideration bubble expansion in the column and neglecting bubble coalescence and breakup. In particular, the model can be applied to tall flotation columns in mineral processing industries where the column operates in the homogeneous regime and bubble expansion along the column height is significant. The model essentially captures the effect of superficial gas velocity, superficial liquid velocity, bubble rise velocity, operating pressure, and column height on the average gas holdup. An axial profile of gas holdup is also obtained. The predictions of this model are in excellent agreement with the experimental data available from the literature.

(2) Axial variation of mean bubble diameter and the gas holdup in the froth is addressed by considering the steady-state coalescence process from a probabilistic perspective and considering a constant transition probability for bubble coalescence.

Notation

b = constant defined by Eq. 3, dimensionless
d_B = bubble diameter, m
$f_1(x, z)$ = number density of bubbles of volume x at location z, m^{-6}
g = acceleration arising from gravity, m/s^2
H = height of gas–liquid dispersion, m
H_0 = height of liquid column, in the absence of gas flow, m
H_a = pressure head acting on the top of the column, m
m = Richardson–Zaki index, dimensionless
N_0 = number of bubbles per unit volume, m^{-3}
u_L = interstitial liquid velocity, m/s
x = bubble volume, m^3
$\dot{X}$ = rate at which bubble volume increases, m^3/s
V_G = superficial gas velocity, m/s
V_L = superficial liquid velocity, m/s
V_S = slip velocity, that is, relative velocity between bubbles and liquid, m/s
z = axial location in the column, m
$\dot{Z}$ = bubble rise velocity with respect to stationary coordinates, m/s

Greek letters

β = transition probability for bubble coalescence, m^3/s
δ = Dirac-delta function
ϕ_0 = gas holdup at the sparger region, dimensionless
$\in_G$ = gas holdup, dimensionless
$\overline{\in}_G$ = average gas holdup, dimensionless
$\in_L$ = liquid holdup, dimensionless
$\overline{\in}_L$ = average liquid holdup, dimensionless
ρ_G = gas density, kg/m^3
ρ_L = liquid density, kg/m^3

Literature Cited

1. Deckwer WD. Bubble Column Reactors. 2nd Edition. Chichester, UK: John Wiley & Sons; 1992.
2. Clift R, Grace JR, Weber ME. Bubbles, Drops, and Particles. New York: Academic Press; 1978.
3. Hulburt HM, Katz SL. Some problems in particle technology: A statistical mechanical formulation. *Chem Eng Sci*. 1964;19:555–574.
4. Randolph AD, Larson MA. A population balance for countable entities. *Can J Chem Eng*. 1964;42:280–281.
5. Ramkrishna D. The status of population balances. *Rev Chem Eng*. 1885;3:49–95.
6. Ramkrishna D. Population Balances Theory and Applications to Particulate Systems in Engineering. San Diego, CA: Academic Press; 2000.
7. Yianatos JB, Finch JA, Laplante AR. Holdup profile and bubble size distribution in flotation column froths. *Can Metall Q*. 1986;25:23–29.
8. Richardson JF, Zaki WN. Sedimentation and fluidization: Part I. *Trans IChemE*. 1954;32:35–53.
9. Mendelson HD. The prediction of bubble terminal velocity from wave theory. *AIChE J*. 1967;13:250–252.
10. Gomez CO, Uribe-Salas, Finch JA, Huls BJ. Gas hold-up measurement in flotation columns using electrical conductivity. *Can Metall Q*. 1991;30:201–205.
11. Zhou ZA, Egiebor NO. Prediction of axial gas holdup profiles in flotation columns. *Miner Eng*. 1993;6:307–312.
12. Yianatos JB, Bergh LG, Sepulveda C, Nunez R. Measurement of axial pressure profiles in large-size industrial flotation columns. *Miner Eng*. 1995;8:101–109.
13. Wilkinson PM. Physical Aspects and Scale-up of High Pressure Bubble Columns. PhD Thesis. Groningen, The Netherlands: University of Groningen; 1991.
14. Letzel M. Hydrodynamics and Mass Transfer in Bubble Columns at Elevated Pressures. PhD Thesis. Delft, The Netherlands: Delft University; 1998.
15. Joshi JB, Deshpande NS, Dinkar M, Phanikumar DV. Hydrodynamic stability of multiphase reactors. *Adv Chem Eng*. 2001;26:1–130.
16. Schugerl K, Oels U, Lucke J. Bubble column bioreactors. *Adv Chem Eng*. 1977;7:1–84.
17. Finch JA, Dobby GS. Column Flotation. Oxford, UK: Pergamon Press; 1990.
18. Xu M, Finch JA. Effect of sparger surface area on bubble diameter in flotation columns. *Can Metall Q*. 1989;28:1–6.
19. Ramkrishna D, Borwanker JD. A puristic analysis of population balance—I. *Chem Eng Sci*. 1973;28:1423–1435.

Manuscript received Mar. 07, 2006, and revision received Oct. 20, 2006.